Am J Transl Res 2019;11(3):1403-1416
www.ajtr.org /ISSN:1943-8141/AJTR0091233

*Original Article*

# Prevascularized mesenchymal stem cell-sheets increase survival of random skin flaps in a nude mouse model

Fei Zhou[1], Lijun Zhang[1], Lei Chen[1], Yingbin Xu[1], Yanan Chen[1], Zilun Li[2], Xusheng Liu[1], Jun Wu[1], Shaohai Qi[1]

[1]*Department of Burns Surgery, First Affiliated Hospital of Sun Yat-sen University, Guangzhou, Guangdong, China;* [2]*Department of Vascular Surgery, First Affiliated Hospital of Sun Yat-sen University, Guangzhou, Guangdong, China*

Received January 13, 2019; Accepted January 23, 2019; Epub March 15, 2019; Published March 30, 2019

**Abstract:** A random skin flap is commonly applied in plastic and reconstructive surgery. The distal part of the random skin flap often risks necrosis because the blood flow may be compromised. Prevascularization is a widely used technology to intensify the vascularization function of biomaterials. In fact, human mesenchymal stem cell (hMSC) sheets promote neoangiogenesis. We speculated that prevascularized hMSC cell sheets (PHCS) would further improve neovascularization by producing more angiogenic growth factors in a random skin flap animal model. In this study, PHCS were set up by co-culturing human umbilical vein endothelial cells (HUVECs) with hMSC cell sheets (HCS). *In vitro*, we observed microvessel formation and significantly increased production of angiogenesis-related factors. Thus, we analyzed the microvessel networks, vascular maturation, and angiogenic growth factors of the cell sheet. *In vivo*, PHCS and HCS were implanted in a murine ischemic random skin flap model. Implanted PHCS significantly increased blood perfusion and improved skin flap survival when compared to untreated control skin flaps. The survival rate of the prevascularized and control skin flaps was assessed after 3, 5, and 7 days via analysis of macroscopic images and Laser Doppler Perfusion Imaging (LDPI). Additionally, the numbers of skin appendages, collagen fibers deposition, and epidermal thickness were evaluated. Moreover, the PHCS group also induced the most intense neovascularization, the upshot of which was a robust blood microcirculation supporting skin flap survival. Therefore, PHCS implantation can effectively enhance local neoangiogenesis and hence increase the survival of otherwise ischemic skin flaps. Hence, local administration of PHCS may serve as an alternative approach in improving random skin flap survival.

**Keywords:** Skin flap, human mesenchymal stem cell, prevascularized cell sheet, angiogenic growth factors

## Introduction

Random skin flaps are a common treatment method in plastic and reconstruction surgery, especially in small to medium size wounds [1]. Because the flap blood supply only gets through the pedicle part, after surgery, the distal part is exposed to ischemia and hypoxia conditions before micro vessel connections are available to the wound bed [2]. Due to the risk of ischemic condition, the flaps have a flap length to width ratio of 2:1 to 3:1 depending on the site and surgeon. An excessive flap length should be avoided because the distal blood flow may become insufficient, thereby risking distal flap necrosis [3]. Although plastic surgeons take several measures to improve survival of the skin flap, distal flap necrosis is still a major complication, which results in secondary surgical operations thus delaying further therapies [4].

Therefore, novel technological approaches endowed with greater therapeutic effectiveness are of the utmost importance. When treating ischemic tissues, including skin flaps, it is important to improve the local neovascularization. In recent years, studies have mainly focused on growth factors administration [5], angiogenesis-inducing gene transfection [6], and cell therapies [7, 8]. Cell therapies, especially those involving stem cells, have been developed as a novel strategy to accelerate the neovascularization of ischemic tissue. Stem cells possess both the ability to differentiate into multiple cell lineages and the potential to secrete various growth factors and/or cytokines, which can exert a beneficial therapeutic

effect on the ischemic tissue [9-11]. Existing lines of evidence have indicated that mesenchymal stem cells (MSCs) may usefully improve the survival of ischemic skin flaps. Local delivery of rat adipose-derived MSCs to random pattern skin flaps led to a significant increase in flap viability [4, 12]. It has also been proven that cytokines and growth factors secreted by stem cells promote *in vivo* neoangiogenesis in ischemic tissues through a paracrine mechanism [4, 12]. However, the implantation of MSCs has its limits because of their rather poor survival within ischemic tissues [13]. Traditional delivery routes, such as injecting or spraying a cell suspension, have drawbacks, including a lack of control as to where cells end up and a non-homogeneous distribution of the cells within the treated area [14]. Engineering of cell sheets can prevent such risks and preserve the extracellular matrix, cell-cell junctions, and cell-matrix links, thereby restricting the cells to the treated area [15]. *In vivo* studies have already proven that cell sheets can provide a better long-term tissue survival as compared to the injection of a cell suspension [16]. Notably, the implantation of MSCs cell sheets increased the survival area of random skin flaps due to the increased expression of angiogenic factors [17].

Recent advances in tissue engineering have led to better strategies aimed at improving the beneficial therapeutic effects of cell sheets. One of the most widely used strategies has involved prevascularization methods [18]. Previous formation of a functional microvessel network on cell sheets may promote angiogenesis and further improve tissue function [19]. Among all cell types used on angiogenesis studies, endothelial cells have been widely applied on different types of matrices to produce vascular networks [20, 21]. When co-cultured with hMSCs, endothelial cells will increase the amount of released angiogenic growth factors driving the maturation and stabilization of newly formed vascular structures [22]. In rats, prevascularized cell sheets exerted superior beneficial therapeutic effects as compared to other cell sheet types when applied to a full thickness wound model have [23]. Hence, prevascularized cell sheets will improve skin flap survival by accelerating local neoangiogenesis.

The aim of this study was to assess the effectiveness of prevascularized HCS to accelerate neovascularization and increase skin flap survival. In brief, hMSC sheets were first cultured under hypoxia, and next co-cultured with HUVECs under normoxia to induce the formation of a more extended and more intricate microvessel network [24]. After that, both the vascularized and non-vascularized cell sheets were applied together with random skin flaps to skin wounds and the microvessel network, vascular maturation, and angiogenic growth factors released from the cell sheets were analyzed. The survival rate of skin flaps was evaluated after 3, 5, and 7 days by microscope images and LDPI analysis. Additionally, the number of skin appendages, collagen fiber accumulation, epidermis thickness, and vessels density were assessed.

## Materials and methods

### *Culture of prevascularized hMSC cell sheets*

The cell sheet cultivation method used was as previously described [24]. In this study, we adopted the optimized culture condition for PHCS and HCS. Passages 3 to 5 hMSC (Sciencell, San Diego, CA, USA) were seeded at $10^4$ cells/cm$^2$ on cover glasses coated with 20 μg/ml collagen I (BD Biosciences, San Jose, CA, USA). To obtain HCS, hMSCs were cultured for 28 days in a hypoxia chamber (BioSpherix, Lacona, NY, USA) flushed with a gas mixture of the following composition: 2% $O_2$-5% $CO_2$-93% $N_2$ v/v. hMSCs were incubated with α-Minimum Essential Medium fortified with 20% fetal bovine serum, 1% L-glutamine, and 1% penicillin/streptomycin (Life Technologies, Rockville, MD, USA). To produce prevascularized hMSC cell sheets (PHCS), HUVECs (Sciencell, San Diego, CA, USA) were seeded on top of hMSC cell sheets at a density of $2\times10^4$/cm$^2$ and cultured under a normoxic conditions (20% $O_2$) for 2 weeks in endothelial cell medium (ECM, Sciencell, San Diego, CA, USA). The medium was changed every other day.

### *Microvessels staining and quantification*

The amount of developed vasculature was measured via immunofluorescent staining. Cell sheets were washed with phosphate-buffered saline (PBS), fixed in 4% paraformaldehyde (PFA), blocked with 2.0% bovine serum albumin

(BSA) (Sigma, St. Louis, MO, USA) in 0.2% Triton X-100 (Sigma, St. Louis, MO, USA) for 30 minutes at room temperature. The incubation with mouse anti-human CD31 monoclonal antibody (BBA7, R&D Systems, Minneapolis, MN, USA) overnight at 4°C was followed by an incubation with anti-mouse IgG (H + L) F(ab')2 fragment (Alexa Fluor® 488 Conjugate) (Cell Signaling Technology, Danvers, MA, USA) also for 1 hour at room temperature. Nuclei were stained with a solution of 4',6-diamidino-2-phenylindole (DAPI, 1:1000, Thermo Fisher Scientific, Waltham, MA, USA). Low-magnification (5× objective) images were acquired with a fluorescent microscope (Leica 6B, Leica, Wetzlar, Germany), combined with a LAS (Leica application suite) X suit. Five images of the microvessel networks pertaining to three individual samples per group were combined and processed with Angiotool software [25].

*Basement membrane staining and permeability assay*

Staining of basement membrane collagen IV was performed on 4% PFA fixed cell sheets which were next blocked with 2% BSA in PBST for 1 h at room temperature, and then treated overnight at 4°C with anti-collagen IV antibody (ab6586, 1:200, Abcam, Cambridge, MA, USA). Staining was visualized after incubation for 1 h at room temperature with anti-rabbit 557 antibody (1:400; R&D systems, Minneapolis, MN, USA). Procedures for staining nuclei and acquiring images were the same as above described. For permeability assay, cell sheets were incubated at 37°C for 30 minutes with a 5% 70 kDa Texas Red-conjugated dextran (Thermo Fisher Scientific Life Sciences, Waltham, MA, USA) in PBS, and excess dextran was removed by washing in PBS [26]. Next assay procedures were completed by fixation, anti-CD31 staining, and confocal imaging (LSM780; Zeiss, Oberkochen, Germany) as above described.

*Human proteome profiler antibody array of conditioned medium*

The cell culture medium was sampled from HCS and PHCS on day 7 and 14 after co-culturing with ECM. The human angiogenesis array (ARY007, R&D systems, Minneapolis, MN, USA) was performed according to the manufacturer's instructions. Quantitative analyses were carried using GenePix Pro (San Jose, CA, USA).

*Animals*

All experimental procedures were conducted according to the First Affiliated Hospital of Sun Yat-sen University Institutional Animal Care and Use Committee guidelines (Guangzhou, Guangdong, China). Male Balb-c/nu mice, weighing 20-24 g were obtained from the Nanjing Biomedical Research Institute of Nanjing University. Mice were randomly divided into three groups according to the different surgical treatment: control, HCS, and PHCS. Each group consisted 20 mice (i.e., 5 mice per time point).

*Ischemic skin flap model and cell sheet implantation*

Balb/c-nu mice underwent gas anesthesia (isoflurane, 2% v/v in $O_2$ 98% v/v, 2 L/min) prior to surgery. During the operation, aseptic techniques were maintained by providing a local sterile environment in a specific pathogen-free (SPF) animal lab.

After an adequate degree of anesthesia was reached, animals were put on an operating table with their limbs extended. A random pattern skin flap having a size of 0.5×2.5 cm (1:5) was cut on each mouse dorsum by using a scalpel, the depth of which was extended to a plane superficial to the deep muscular fascia. Thus, the skin flap was made of the skin, superficial fascia, panniculus carnosus, and subcutaneous connective tissue. The flap did not include any axial vessels, which resulted in the flap pedicle distal end being ischemic. For cell sheet implantation, once the proximal half of the flap was sutured with intermittent stitches, the cell sheet was laid upon the sarcolemma. After sufficient hemostasis was achieved, the distal half of the flap was sutured back into place with 5-0 running stitches. After surgery, the animals were housed in separate cages.

*Assessment of skin flap surviving areas and blood perfusion*

At 0, 1, 3, 5, and 7 day after surgery, pictures of the dorsal skin flap were taken always in the same spot using a digital camera. The extent of the surviving areas of skin flaps was blindly assessed by two surgeons taking stock of color changes, eschars, and non-epithelialized area as compared with flap features of the control mice group. At each time point of sampling,

ImageJ software (National Institutes of Health, Bethesda, MD, USA) was used to measure the percentage of the surviving areas in relation to the total surface area of the flaps.

The amount of blood perfusion of the skin flaps was evaluated at each time point using a LDPI system (PeriScan PIM3, Perimed, Stockholm, Sweden). In brief, mice were positioned in a similar fashion as for the making of the skin flap with appropriate anesthesia. The probe scanned dorsal skin flap surface at least for 30 seconds, and the results were recorded as blood relative perfusion units (RPU). Contrast images were processed to display a color-coded live flux image. During blood flow measurements, the temperature of the heating pad was steadily kept at 37°C. In order to accurately quantify the extent of ischemic areas, the latter were identified as regions having an RPU value < 100.

*Tissues sampling*

Mice were sacrificed at 3, 5, 7 days after the operation. The skin flaps and nearby tissues were picked up and directly split into two portions along the centerline. Next, both parts of each sampled skin flap s were fixed with 4% PFA and stored in liquid nitrogen (-196°C). When devised, the fixed tissues were dehydrated and embedded in paraffin.

*Histological and immunofluorescent analysis*

*Histology:* Tissue sections (5-μm thick) were cut from paraffin blocks using a microtome (Shandon Finesse 325, Thermo Fisher Scientific Life Sciences, Waltham, MA, USA) and next deparaffinated and rehydrated prior to be used for staining. Hematoxylin and eosin (HE) staining and Masson's Trichrome staining were performed following the manufacturer's guidelines [23]. The collagen fibers accumulation level, expressed as the collagen index (CI) was computed for each pixel within the images of interest according to the equation:

$$CI = (B + G)/(2R + B + G)$$

Where R, B, and G represented the red, blue, and green pixel values, respectively. The value of the CI ranged from 0 for extremely red objects to 1 for completely blue-green objects [16, 17]. Four stained sections per each group and per time point were visualized using a KF-PRO-005 digital platform (Konfoong Biotech International CO., LTD, NingBo, China). For quantitative analysis, three random fields were selected in each section.

*Immunofluorescence:* Anti-CD31 staining: The skin flap samples were taken out of liquid nitrogen, placed in OCT (Thermo Fisher Scientific Life Sciences, Waltham, MA, USA), and next cut into 10-μm thick sections in a microtome (Shandon Cryotome FSE, Thermo Fisher Scientific Life Sciences, Waltham, MA, USA). Sections were blocked with 2% BSA in PBS Tween-20 (PBST) for 1 hour at room temperature, and next incubated overnight at 4°C with rat anti-CD31 antibody (ab7388, 1:400; Abcam, Cambridge, MA, USA) and visualized with anti-rat IgG H&L (1:400; Alexa Fluor® 647; Abcam, Cambridge, MA, USA) applied for 1 hour at room temperature. Procedures for nuclear staining and section images were performed as described above.

*Cell tracking in vivo*

For *in vivo* short-term tracking, hMSCs were labeled with CM-DiI (Invitrogen, Carlsbad, CA, USA) according to the manufacturer's instructions. HUVECs were labeled with CFSE (Molecular Probes, Leiden, Netherlands) according to the manufacturer's instructions and then incubated with hMSCs for 14 days, and then administrated with skin flap model or subcutaneous implant model for another 7 days. The samples were extracted and embedded in OCT. Finally, acquired sections were stained with DAPI and then observed under a fluorescent microscope (Leica 6B, Leica, Wetzlar, Germany).

*Statistics/data analysis*

Results are presented as mean values ± standard deviation. Statistical comparisons between two groups with t-tests or among greater than two groups with a one-way ANOVA. Results differences were considered statistically significant when $P < 0.05$.

## Results

*Microvessel network formation on prevascularized cell sheets in vitro*

Co-culture of HUVECs and hMSC cell sheets exhibited reproducible network formation by

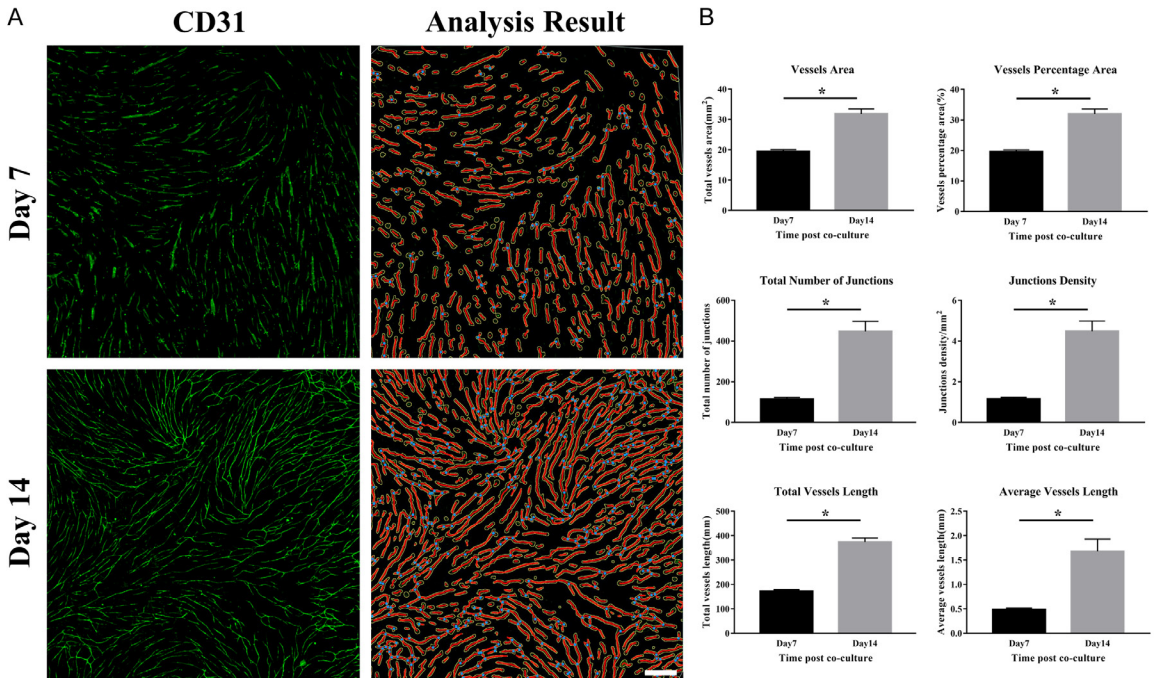


**Figure 1.** Complex microvessel network formation of PHCS at day 7 and 14. A. Mosaic image of CD31 (green) Immunofluorescence staining and analysis result with Angiotool (yellow: vessel outline, red: skeleton, blue: branch points). B. Quantitative analysis of microvessel networks of prevascularized cell sheets. *$p < 0.05$. Bar: 1 mm.

the endothelial cells. Cultures using only HUVECs did not lead to any network formation [24]; instead the cells grew as a monolayer. The network formed by HUVECs was confirmed by immunofluorescence staining with anti-CD31 antibody (**Figure 1A**). During a two-week period, HUVECs underwent an expected series of morphological transformations which resulted in a uniform, stable, and interconnected network. This type of microvessel network was observed throughout the culture system and was steadily maintained for 14 days. We also quantitatively characterized the microvessel network (**Figure 1B**). By day 14, the total vessel length per field (9.82 mm × 9.82 mm) was 374.06 ± 36.25 mm, which was much longer than that by day 7 (172.14 ± 15.12 mm). The vessel surface area (day 14: 31.82 ± 3.65 $mm^2$ versus day 7: 19.44 ± 1.38 $mm^2$) and the total number of branch points (day 14: 447.00 ± 111.131 versus day 7: 114.80 ± 18.49) showed the same trend (**Figure 1B**). We combined the cell sheet microscopic images to observe at day 14 the PHCS as a whole, and to visualize the uniform and complex microvessel structure (Figure S1A). Moreover, the morphology of the lumen of PHCS was studied using a 63× objective (Figure S1B).

*Permeability and maturation of microvessel*

Immunofluorescence staining was performed using an antibody against collagen type IV, which is one of the major structural components of vascular basement membranes [27]. Collagen IV was robustly expressed around the HUVECs, and the vessels luminal structure could be observed in the single channel image of collagen IV (**Figure 2A**). Next, we used Texas Red-conjugated dextran to evaluate the permeability with which the microvessels formed within our PHCS at day 14. The dextran tracer was uniformly distributed throughout the extracellular matrix, while the signal was significantly lower in the CD31 positive regions (**Figure 2B**).

*Angiogenic profiling of HCS and PHCS*

The release of angiogenic growth factors from HCS and PHCS into the culture medium was evaluated by means of a human angiogenesis antibody array. Based on the intensity of the positive dots, the three growth factors exhibiting the greatest differences detectable in PHCS vs. HCS included Leptin, Ang2, and PlGF (**Figure 3**).

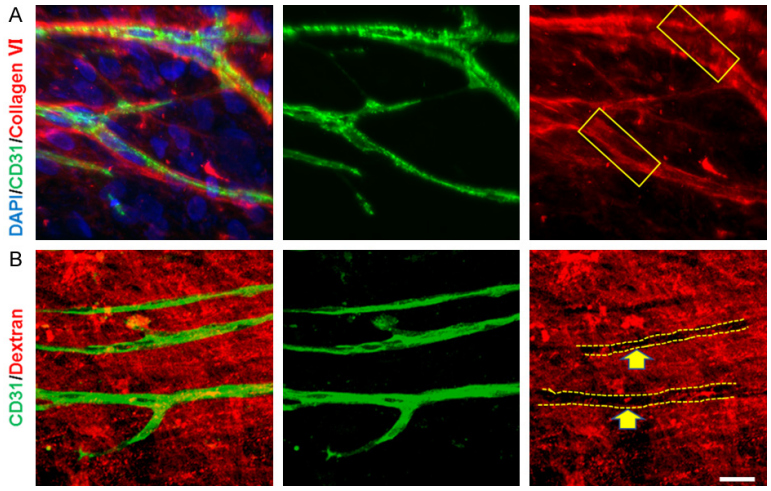


**Figure 2.** Microvessel maturation of PHC. A. CD31 (green) and collagen IV (red) staining of PHC at day 14, and the latter showing the basement membrane (yellow box) formed around the HUVECs. B. Dextran permeability assay of PHCS at day 14. Some low dextran (red) signal regions (yellow arrow and dashed line) formed in the microvessel (green) regions. Bar: 10 μm.

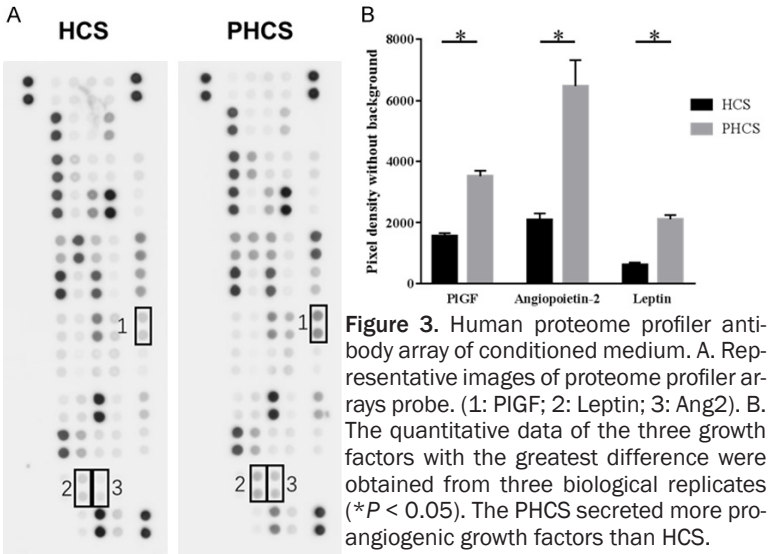


**Figure 3.** Human proteome profiler antibody array of conditioned medium. A. Representative images of proteome profiler arrays probe. (1: PlGF; 2: Leptin; 3: Ang2). B. The quantitative data of the three growth factors with the greatest difference were obtained from three biological replicates (*$P$ < 0.05). The PHCS secreted more pro-angiogenic growth factors than HCS.

*Therapeutic effects of cell sheets for the skin flaps*

Skin flap survival in mice treated with PHCS, HCS or with no treatment was checked over 7 days. Representative images of skin flaps at various time points are presented in **Figure 4A**. In contrast to the control group, the crusta in the PHCS group and HCS group was inconspicuous during the early stage after surgery. The relative skin flap survival rate was expressed as the percentage of surviving area with respect to the entire surface of the skin flap. A lower survival rate indicated that a severe ischemia had caused skin flap tissue necrosis, which may have resulted in a poor clinical outcome. When compared to the control group at day 3 and 5, PHCS and HCS showed a therapeutic effect on the skin flap tissue survival. Notably, the PHCS group exhibited a better survival rate than the HCS group. At day 7, there occurred still significant differences in percent flap survival between the PHCS group and the other two groups (84.678 ± 2.420% versus 77.923 ± 3.639% and versus 75.273 ± 3.493%, respectively; $P < 0.05$ in either instance). No statistically significant differences were observed between the HCS group and control group ($P>0.05$; **Figure 4B**).

*Blood perfusion of skin flaps*

On postoperative day 1, 3, 5, and 7, the blood perfusion of the skin flaps was evaluated by LDPI analysis. The mean value of skin flaps relative perfusion units (RPU) was significantly different between the PHCS group and the control group at day 1 (**Figure 5**) (102.122 ± 3.996 versus 85.716 ± 5.905; $P < 0.05$), and at day 5 (122.89 ± 10.654 versus 102.752 ± 4.48; $P < 0.05$). As regards the extent of the ischemic areas, significant differences were observed especially at day 3 between the PHCS group and the control group (**Figure 5**; 42.120 ± 5.205 $mm^2$ versus 25.785 ± 1.575 $mm^2$, $P < 0.05$). Conversely, no significant differences were detected between the HCS group and the control group. These findings showed that PHCS promoted the recovery of blood perfusion and decreased the extent of the ischemic areas of the skin

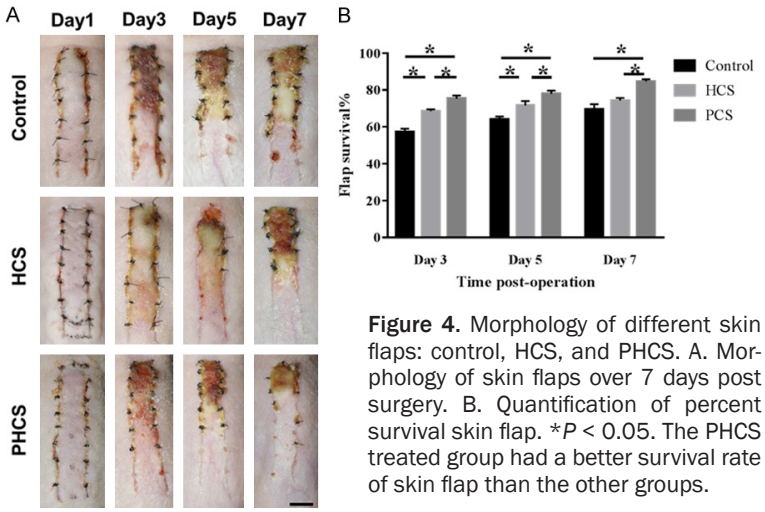


**Figure 4**. Morphology of different skin flaps: control, HCS, and PHCS. A. Morphology of skin flaps over 7 days post surgery. B. Quantification of percent survival skin flap. *$P < 0.05$. The PHCS treated group had a better survival rate of skin flap than the other groups.

flaps, especially at the early stages post-operation.

*Histological changes*

Tissue sections collected from the distal one half portion of each skin flap underwent HE staining to characterize microstructural and cellular changes occurred at day 3, 5, and 7. Thus, at day 3 in comparison with the PHCS and HCS groups, the skin flaps from the control group exhibited a thinner dermis with numerous necrotic skin appendages. Conversely, abundant normal-looking skin appendages were detected in the HCS groups. At day 5, the remaining tissue was found to be necrotic in the control and HCS groups, whereas in the PHCS group significantly less eschar tissue could be observed. The epidermis in the control and HCS groups started to come out under the eschar, whereas in the PHCS group more maturation structures were found. At day 7, the PHCS group presented with a more regular histology of the epidermis which was endowed with a higher number of skin appendages (PHCS 13.5 ± 1.291 versus HCS 6.25 ± 1.708 and control 1.25 ± 1.5, respectively, $P < 0.05$).

The morphological features of the dermis and the epidermal thickness were further characterized and are presented in **Figure 7**. The morphology of the dermis was analyzed in Masson's trichrome stained sections, in which the blue shaded areas represent the collagen fibers. As shown in **Figure 7A**, the control group exhibited an immature collagen (light blue color), which at day 7 surrounded the fibroblasts, whereas collagen fibers were still in an admixed naive state in the HCS group: conversely, organized mature collagen could be observed in the PHCS group. Quantitative image analysis (**Figure 7B**) demonstrated that the collagen index (CI; the intensity of collagen fibers accumulation) in the control (0.507 ± 0.011) and HCS (0.553 ± 0.011) groups was lower as compared to that in normal skin (0.639 ± 0.014). Notably, the CI in the PHCS group (0.609 ± 0.006) was very close to the normal skin level.

*Analysis of vessels density*

To confirm the therapeutic effects elicited by promoting the neovascularization, the expression of the vascular endothelial cell marker CD31 was analyzed (**Figure 8**). An improved neoangiogenesis was observed in the PHCS group as compared with the control group at all time points as measured by the respective values of the CD31 areas ($\mu m^2$/microscopy field at 20× magnification: day 3, 9199.00 ± 2391.44 versus 2998.80 ± 1120.97; day 5, 15608.40 ± 4422.288 versus 7519.20 ± 1119.08; 23168.40 ± 6829.40 versus 13029.20 ± 1491.93, respectively, $P < 0.05$ in all instances). Conversely, no statistical difference occurred between the HCS and the control group.

*Cell tracking in vivo*

On day 7 after implantation of cell sheets, we could not trace the stem cells of the cell sheets within the skin flap animal model. In the subcutaneous implantation animal model, fluorescent microscopic examination showed the CM-Dil-labeled hMSCs and CFSE-labeled HUVEC in each specimen we examined (Figure S2).

## Discussion

The therapeutic effects of cell sheets can be significantly improved by a prevascularization procedure *in vitro* and *in vivo* [28-30]. In this study, prevascularized hMSC cell sheets were bio-fabricated according to our previous cell-sheet protocol [24]. Observation by immunofluorescence staining of the, the microvessel structure *in vitro* revealed that the PHCS group could form a uniform and complex microvascular network by day 14 of co-culture. In a next

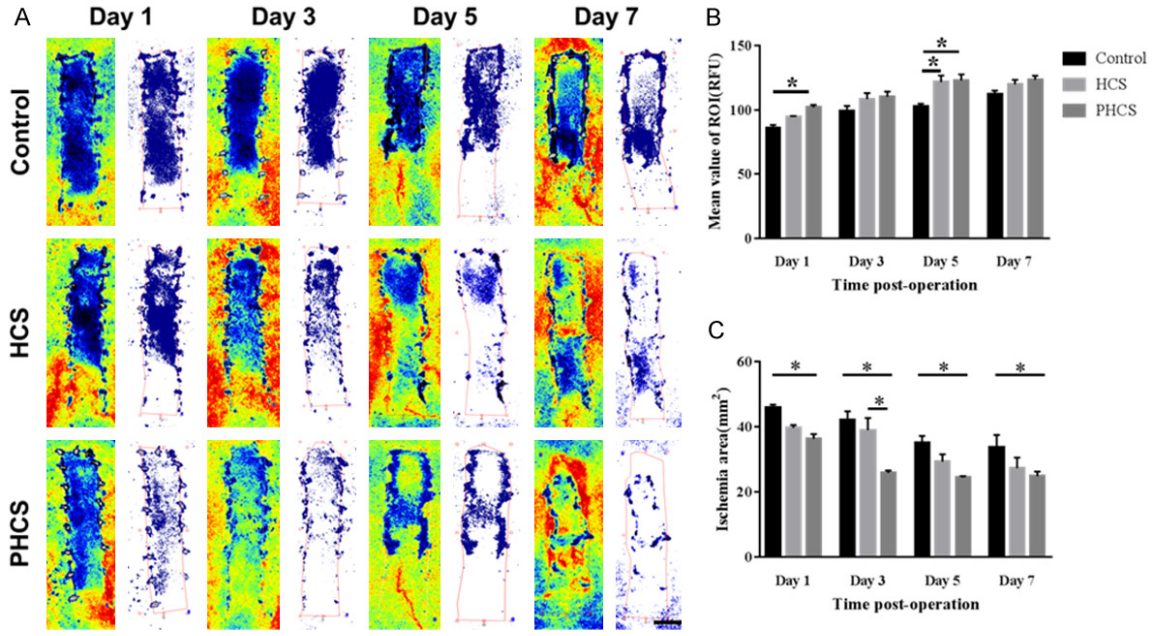


**Figure 5.** Laser doppler perfusion image analysis. A. Representative LDPI images obtained on post-operation day 1, 3, 5, and 7. In multiple color-coded images, high blood flow is depicted in red, while low perfusion is displayed as blue to dark blue. In blue-white images, blood flow lower than 100RFU is depicted in blue. Bar: 5 mm. B. Mean blood flow perfusion of flaps of three groups. *$P < 0.05$. C. Ischemic area of skin flaps of three groups. *$P < 0.05$. PHCS promoted the recovery of blood perfusion, and decreased ischemic areas of the skin flaps.

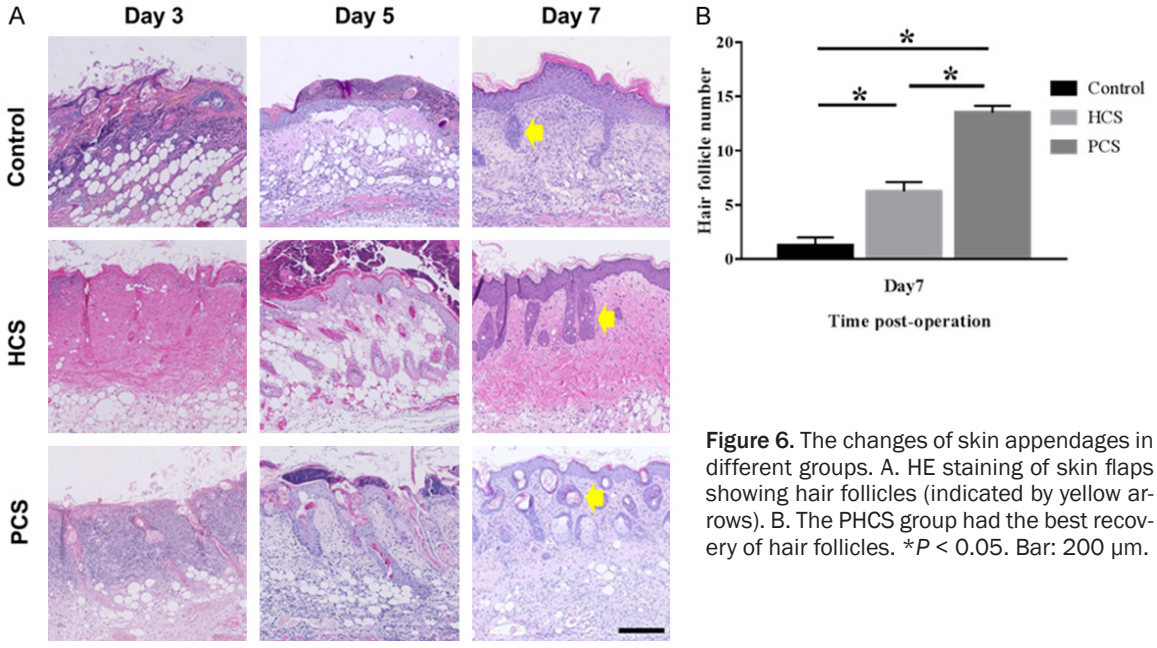


**Figure 6.** The changes of skin appendages in different groups. A. HE staining of skin flaps showing hair follicles (indicated by yellow arrows). B. The PHCS group had the best recovery of hair follicles. *$P < 0.05$. Bar: 200 μm.

step, we evaluated the angiogenic functions of HCS and PHCS in mouse dorsum skin flaps having standard sizes (0.5×2.5 cm). Though the local application of PHCS, the skin flaps survival was markedly advanced as compared with the control and HCS groups as confirmed by the increased blood perfusion in the PHCS group. In addition, the results of both the histological analysis and anti-CD31 immunofluorescence analysis proved the greater therapeutic potential of the PHCS group.

Except for the observation of the microvessel network, we also proved that the PHCS group

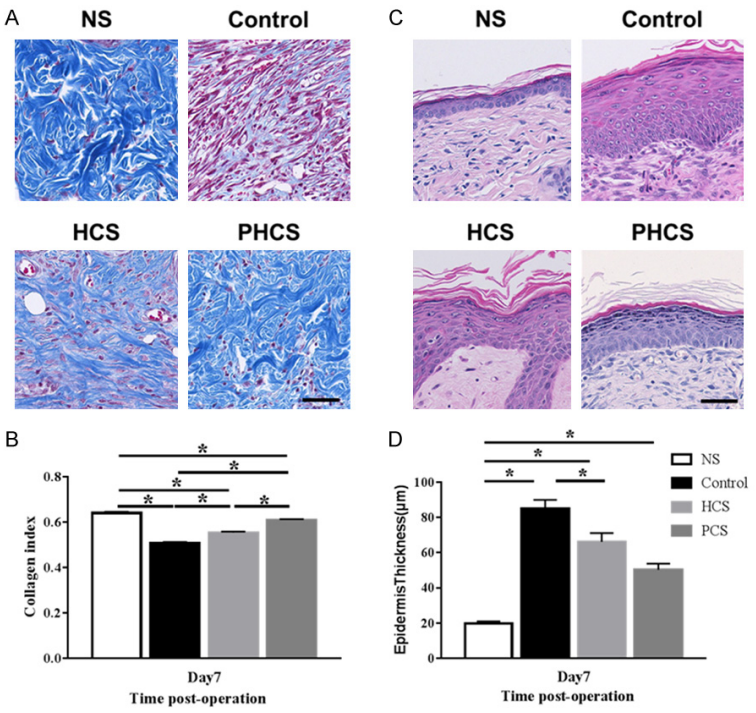


**Figure 7.** Morphological changes of epidermis and dermis in the normal skin and skin flaps. A. Masson's trichrome staining on post operative day 7. Bar: 50 μm. B. Quantification of collagen intensity in the image. *$P < 0.05$. C. HE staining of epidermis. Bar: 50 μm. D. Thickness of epidermis on day 14 and 28. *$P < 0.05$. In the PHCS group, the morphological features of epidermis and dermis are very close to those proper of normal skin.

had the potential to promote the formation of mature microvessels. The latter were surrounded by a basement membrane made up mainly of collagen IV, which promoted endothelial cell survival, and helped maintain microvessel steadiness [31]. Specific immunofluorescence staining showed that collagen IV was robustly expressed around the HUVECs after a 14-day co-culture. This finding is indicative of microvessel maturation and basement membrane formation. In addition, we established a model of microvessel permeability. Mature microvessels are impermeable to dextran having a molecular weight higher than 65 kDa. Therefore, we chose a dextran with a molecular weight of 70 kDa [32]. Our results show that the microvessel network had secure cell-cell junctions, which prevented the dextran from freely diffusing into the vessels lumina. Angiogenesis and vascular organization are processes that proceed along multiple stages. Multiple angiogenic growth factors are involved the control of the microvessel network formation, maturation, and correct patterning [33]. The possible mechanisms involved in angiogenesis are related to factors which promote microvessel formation *in vitro* [34].

The angiogenic growth factors perform an important regulatory role in the process of prevascularization *in vitro* [35]. We analyzed the growth factors released into the supernatant of the PHCS and HCS groups to investigate their angiogenic ability. When compared to HCS, the PHSC group secreted higher levels of leptin, placental growth factor (PlGF), and angiopoietin-2 (Ang2). Leptin is mainly secreted by adipocytes and is involved in several processes, such as proliferation, inflammation, and angiogenesis [36, 37]. In previous studies, authors have suggested that leptin significantly promoted angiogenesis *in vitro* [38, 39]. In our co-culture system, PlGF may play a critical role in microvessel formation. Moreover, PHCS produced higher levels of PlGF than HCS. PlGF is a pro-angiogenic factor belonging to the VEGF superfamily. PlGF plays an important role in promoting neovascularization, such as tissue ischemia and wound healing [40]. On the other hand, PlGF is upregulated in human endothelial cells (ECs) embedded in 3-D collagen matrices inducing the formation of a capillary-like network [41]. Hence, an increase of PlGF might help promote the sprouting and branching during angiogenesis. Ang2 is mainly secreted and stored by ECs at sites of active vascular remodeling [42]. Additional biological roles of Ang2 include the regulation of endothelial tube formation, neoangiogenesis, ECs migration and ECs viability [43-45]. Therefore, the increased Ang2 level concurred in promoting microvessel maturation and network formation in PHCS.

In this study, our primary goals were to investigate the role of stem cells in neovascularization and whether prevascularization might optimize the therapeutic effect of HCS. Therefore, nude mice were used. Although in some studies using stem cells immunocompetent animals were used [46], in quite numerous nude mice

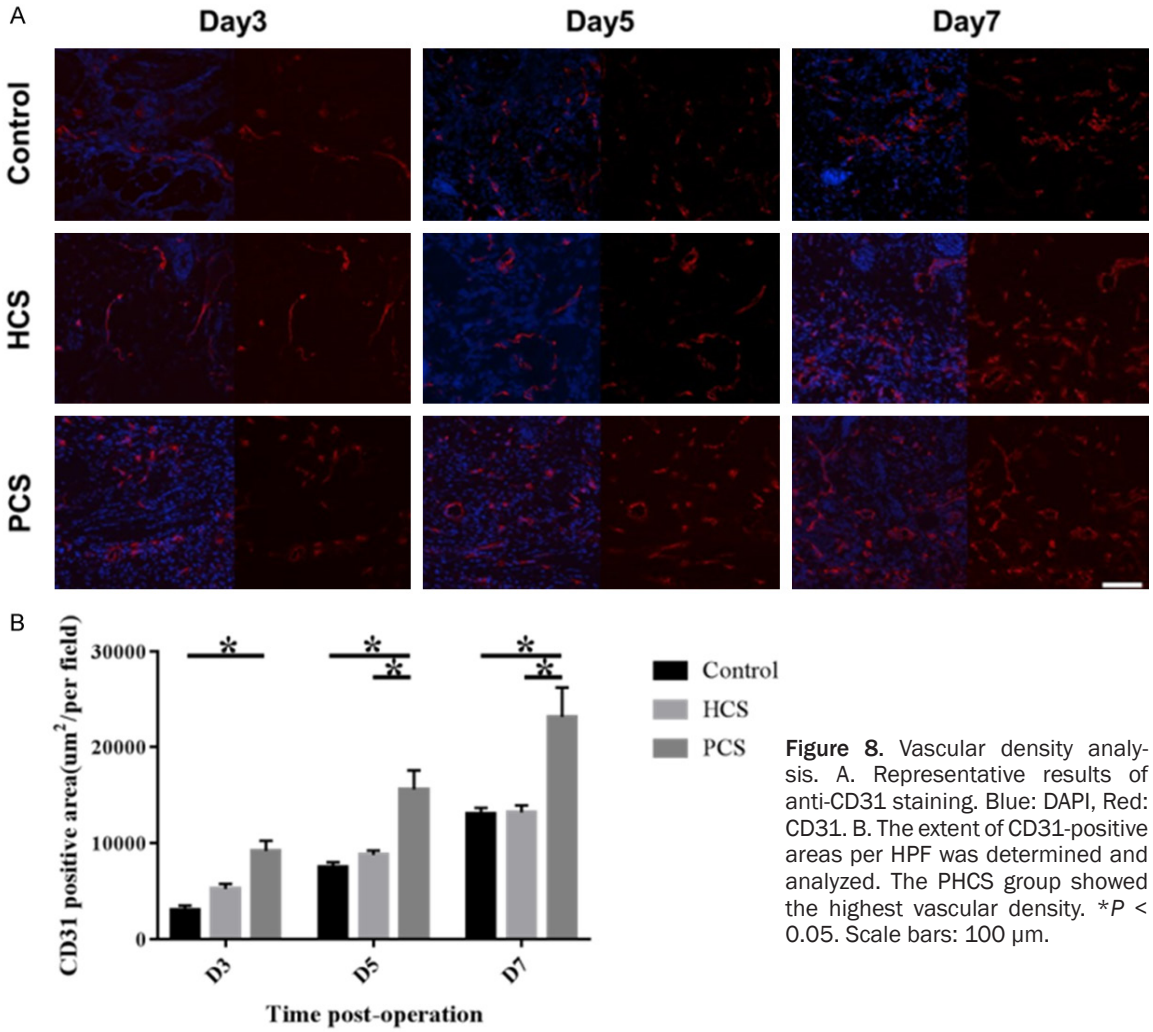


**Figure 8.** Vascular density analysis. A. Representative results of anti-CD31 staining. Blue: DAPI, Red: CD31. B. The extent of CD31-positive areas per HPF was determined and analyzed. The PHCS group showed the highest vascular density. *$P$ < 0.05. Scale bars: 100 μm.

were used to evaluate therapeutic angiogenesis [47]. We selected a nude mice model for our study to diminish the influence of the immune system on the potential therapeutic effects thereby focusing on the role of neovascularization.

To ensure the stability of the ischemic skin flap, we observed the ischemia degree of flaps with different length to width ratios. According to our preliminary findings, for this study we chose a length to width ratio 1:5.

In the early stage after skin flap elevation, the survival and conditions of the skin flaps are crucial for a successful surgical upshot. The distal part of the flap is under ischemic conditions due to an inadequate blood perfusion. Hence, a rapid neovascularization restoring blood perfusion is very important to avoid skin flap necrosis. In our ischemic skin flap animal model, skin flap survival in mice treated with PHCS demonstrated to give superior results over the other groups.

To confirm our preliminary findings, we selected LDPI to evaluate blood perfusion of skin flaps. LDPI is an extension of laser doppler flowmetry that measures capillary blood flow, and has been applied for both clinically and research purposes [48, 49], especially to investigate the microcirculation of skin flaps and to monitor skin flap viability noninvasively [50, 51]. An increase in blood perfusion in the ischemic skin flaps indicated the establishment of an effective microcirculation, capable to supply oxygen and to remove waste products from skin flaps. We found at all time points a significantly higher level of blood perfusion in the PHCS group as compared with the control

group. The PHCS group had the lowest ischemic area at the early stage after flap elevation, which could imply a delayed tissue-protective effect of PHCS.

The normal skin flap has a certain endowment of skin appendages, dermal collagen, and epidermis. For a successful skin flap surgery, it is important to reduce the pathological changes in the early stage and reconstitute the structure and function at the end of the observation. Three days after skin flap elevation, the control group and HCS group showed a significant decrease of normal skin appendages. Moreover, dermal collagen underwent severe necrosis. These pathological features were likely caused by the surgical operation and an inadequate blood supply [52]. When compared to the other two groups, the PHCS group had a better performing dermis at day 3 after surgery. At day 5, naive skin appendages and epidermis sequentially appeared in the control and HCS groups, but the recovery was much slower than in the PHCS group (**Figure 6**). By day 7, the histological appearance was significantly diversified among the groups. The PHCS group, which regained a generally normal appearance, showed a much better recovery than the other two groups as regards CI and epidermis thickness.

Neovascularization is a critical process for skin flap survival, particularly at the early stage of skin flap elevation [53]. The formation of a new microvascular network is a necessary event to restore the supply of oxygen and removal of waste. Our results show that PHCS group had the highest vascularization at all time points, which corresponded to the strongest angiogenic ability. The higher CD31-positive area in the PHCS group indicated the potential to improve the maintenance and viability of skin flaps. Combined with the early pathological results, we speculated that possible reasons for this phenomenon were as follows: firstly, ischemia caused less damage to the skin flap; secondly, a tissue with a milder degree of damage would have a stronger regenerative ability.

In this study, we showed that prevascularization enhanced the therapeutic effect of PHCS in a skin flap model. We speculated that the paracrine effect was a possible mechanism to improve skin flap survival by promoting neovascularization. However, the effect of the stem cells themselves and microvessel structure on the skin flap remains unclear. Using cell tracking technology, we could not trace the stem cells of the cell sheets within the skin flap animal model. The explanations of this may be as follows. First, when compared to the numbers of cells used in the literature, our method used much less cells [12]. However, we still could observe a robust therapeutic effect, which indicated a better function of PHCS. Second, the hypoxic microenvironment of the ischemic skin flap might cause cell apoptosis, resulting in decreased numbers of living cells. A large number of studies selected subcutaneous implantation models for their *in vivo* experiments [54-56], which prevented damage from an ischemic microenvironment. Third, we used a natural material without any scaffold, the physical properties of which were poor. Consequently, the relative mobility between the skin and the muscular layer was higher. However, it is difficult to immobilize cell sheets for a long time. In our subcutaneous implantation model, HUVEC and MSC could be traced at day 7 (Figure S2). This finding supported the above explanations. Further studies will focus on optimizing the cell sheet culture protocol and verify the function of the microvascular structure *in vivo*.

## Conclusion

In this study, we proved that prevascularization strengthened the therapeutic effects *in vitro* and *in vivo* of PHCS, which then secreted increased amounts of pro-angiogenic factors and promoted the formation of mature microvessels *in vitro*. Hence, the implantation of prevascularized PHCS could improve the survival of skin flaps *in vivo*.

## Acknowledgements

We would also like to acknowledge the Experimental Animal Research Laboratory of Sun Yat-sen University for providing experimental animals and the Medical Science Experimentation Center of Sun Yat-sen University for providing the experimental facilities. Supported by Science and Technology Program of Guangzhou (201704020165), Natural Science Foundation of China (NSFC: 81601703), 100 Talents Program of Sun Yat-Sen University (Y61216), “The three and three projects” from The First Affiliated Hospital, Sun Yat-sen University (Y70214).

## Disclosure of conflict of interest

None.

## Abbreviations

BSA, bovine serum albumin; CI, collagen index; EC, endothelial cells; ECM, endothelial cell medium; DAPI, 4', 6-diamidino-2-phenylindole; HCS, hMSC cell sheet; hMSC, human mesenchymal stem cell; HUVECs, human umbilical vein endothelial cells; LAS, Leica application suite; LDPI, laser doppler perfusion imaging; MSCs, mesenchymal stem cells; PBS, phosphate-buffered saline; PFA, paraformaldehyde; PHCS, prevascularized hMSC cell sheet; PlGF, placental growth factor; RPU, relative perfusion units; SPF, specific pathogen-free.

**Address correspondence to:** Shaohai Qi and Jun Wu, Department of Burns Surgery, First Affiliated Hospital of Sun Yat-sen University, Guangzhou, Guangdong, China. E-mail: qishaohaigzburns@163.com (SHQ); junwupro@126.com (JW)

## References

[1] Tønseth KA, Sneistrup C, Berg TM. Prostaglandin E1 increases microcirculation in random pattern flaps on rats measured with laser doppler perfusion imaging. Plast Reconstr Surg Glob Open 2017; 5: e1202.

[2] Baris R, Kankaya Y, Ozer K, Kocer RG, Bektas CI, Karatas A, Kocer U, Koca G, Astarci HM. The effect of microneedling with a roller device on the viability of random skin flaps in rats. Plast Reconstr Surg 2013; 131: 1024-1034.

[3] Huemer GM, Wechselberger G, Otto-Schoeller A, Gurunluoglu R, Piza-Katzer H, Schoeller T. Improved dorsal random-pattern skin flap survival in rats with a topically applied combination of nonivamide and nicoboxil. Plast Reconstr Surg 2003; 111: 1207-1211.

[4] Yue Y, Zhang P, Liu D, Yang JF, Nie C, Yang D. Hypoxia preconditioning enhances the viability of ADSCs to increase the survival rate of ischemic skin flaps in rats. Aesthetic Plast Surg 2013; 37: 159-70.

[5] Uhl E, Barker JH, Bondàr I, Galla TJ, Lehr HA, Messmer K. Improvement of skin flap perfusion by subdermal injection of recombinant human basic fibroblast growth factor. Ann Plast Surg 1994; 32: 361-5; discussion 365-6.

[6] O'Toole G, MacKenzie D, Marucci D, Poole M, Lindeman R, Buckley MF, McCarthy N. Vascular endothelial growth factor gene therapy in ischaemic rat skin flaps. Br J Plast Surg 2002; 55: 55-58.

[7] Cooke JP, Losordo DW. Modulating the vascular response to limb ischemia: angiogenic and cell therapies. Circ Res 2015; 116: 1561-1578.

[8] Boyce ST, Lalley AL. Tissue engineering of skin and regenerative medicine for wound care. Burn Trauma 2018; 6: 4.

[9] Kinnaird T, Stabile E, Burnett MS, Lee CW, Barr S, Fuchs S, Epstein SE. Marrow-derived stromal cells express genes encoding a broad spectrum of arteriogenic cytokines and promote in vitro and in vivo arteriogenesis through paracrine mechanisms. Circ Res 2004; 94: 678-685.

[10] Wen Z, Zheng S, Zhou C, Wang J, Wang T. Repair mechanisms of bone marrow mesenchymal stem cells in myocardial infarction. J Cell Mol Med 2011; 15: 1032-1043.

[11] Wu Y, Chen L, Scott PG, Tredget EE. Mesenchymal stem cells enhance wound healing through differentiation and angiogenesis. Stem Cells 2007; 25: 2648-2659.

[12] Lu F, Mizuno H, Uysal CA, Cai X, Ogawa R, Hyakusoku H. Improved viability of random pattern skin flaps through the use of adipose-derived stem cells. Plast Reconstr Surg 2008; 121: 50-58.

[13] Ohnishi S, Yanagawa B, Tanaka K, Miyahara Y, Obata H, Kataoka M, Kodama M, Ishibashi-Ueda H, Kangawa K, Kitamura S, Nagaya N. Transplantation of mesenchymal stem cells attenuates myocardial injury and dysfunction in a rat model of acute myocarditis. J Mol Cell Cardiol 2007; 42: 88-97.

[14] Segers VF, Lee RT. Biomaterials to enhance stem cell function in the heart. Circ Res 2011; 109: 910-922.

[15] Kirby GTS, Michelmore A, Smith LE, Whittle JD, Short RD. Cell sheets in cell therapies. Cytotherapy 2018; 20: 169-180.

[16] Takeuchi R, Kuruma Y, Sekine H, Dobashi I, Yamato M, Umezu M, Shimizu T, Okano T. In vivo vascularization of cell sheets provided better long-term tissue survival than injection of cell suspension. J Tissue Eng Regen Med 2016; 10: 700-710.

[17] Kira T, Omokawa S, Akahane M, Shimizu T, Nakano K, Nakanishi Y, Onishi T, Kido A, Inagaki Y, Tanaka Y. Effectiveness of bone marrow stromal cell sheets in maintaining random-pattern skin flaps in an experimental animal model. Plast Reconstr Surg 2015; 136: 624-632.

[18] Sekine H, Shimizu T, Hobo K, Sekiya S, Yang J, Yamato M, Kurosawa H, Kobayashi E, Okano T. Endothelial cell coculture within tissue-engineered cardiomyocyte sheets enhances neovascularization and improves cardiac function of ischemic hearts. Circulation 2008; 118: 145-153.

[19] Rivron NC, Liu J, Rouwkema J, De Boer J, Van Blitterswijk CA. Engineering vascularised tissues in vitro. Eur Cells Mater 2008; 15: 27-40.
[20] Pelletier L, Angonin R, Regnard J, Fellmann D, Charbord P. Human bone marrow angiogenesis: In vitro modulation by substance P and neurokinin A. Br J Haematol 2002; 119: 1083-1089.
[21] Korff T, Augustin HG. Tensional forces in fibrillar extracellular matrices control directional capillary sprouting. J Cell Sci 1999; 112: 3249-3258.
[22] Levenberg S, Rouwkema J, Macdonald M, Garfein ES, Kohane DS, Darland DC, Marini R, Van Blitterswijk CA, Mulligan RC, D'Amore PA, Langer R. Engineering vascularized skeletal muscle tissue. Nat Biotechnol 2005; 23: 879-884.
[23] Chen L, Xing Q, Zhai Q, Tahtinen M, Zhou F, Chen L, Xu Y, Qi S, Zhao F. Pre-vascularization enhances therapeutic effects of human mesenchymal stem cell sheets in full thickness skin wound repair. Theranostics 2017; 7: 117-131.
[24] Zhang L, Xing Q, Qian Z, Tahtinen M, Zhang Z, Shearier E, Qi S, Zhao F. Hypoxia created human mesenchymal stem cell sheet for prevascularized 3D tissue construction. Adv Healthc Mater 2016; 5: 342-352.
[25] Zohar B, Blinder Y, Mooney DJ, Levenberg S. Flow-induced vascular network formation and maturation in three-dimensional engineered tissue. ACS Biomater Sci Eng 2018; 4: 1265-1271.
[26] Zhang L, Qian Z, Tahtinen M, Qi S, Zhao F. Prevascularization of natural nanofibrous extracellular matrix for engineering completely biological three-dimensional prevascularized tissues for diverse applications. J Tissue Eng Regen Med 2018; 12: e1325-e1336.
[27] Nillesen ST, Geutjes PJ, Wismans R, Schalkwijk J, Daamen WF, van Kuppevelt TH. Increased angiogenesis and blood vessel maturation in acellular collagen-heparin scaffolds containing both FGF2 and VEGF. Biomaterials 2007; 28: 1123-1131.
[28] Chen L, Xing Q, Zhai Q, Tahtinen M, Zhou F, Chen L, Xu Y, Qi S, Zhao F. Pre-vascularization enhances therapeutic effects of human mesenchymal stem cell sheets in full thickness skin wound repair. Theranostics 2017; 7: 117-131.
[29] Sakaguchi K, Shimizu T, Okano T. Construction of three-dimensional vascularized cardiac tissue with cell sheet engineering. J Control Release 2015; 205: 83-88.
[30] Asakawa N, Shimizu T, Tsuda Y, Sekiya S, Sasagawa T, Yamato M, Fukai F, Okano T. Prevascularization of in vitro three-dimensional tissues created by cell sheet engineering. Biomaterials 2010; 31: 3903-3909.
[31] Carmeliet P. Angiogenesis in health and disease. Nat Med 2003; 9: 653-60.
[32] Curry FE, Huxley VH, Adamson RH. Permeability of single capillaries to intermediate-sized colored solutes. Am J Physiol 1983; 245: H495-505.
[33] Rouwkema J, Khademhosseini A. Vascularization and angiogenesis in tissue engineering: beyond creating static networks. Trends Biotechnol 2016; 34: 733-745.
[34] Bogorad MI, DeStefano J, Karlsson J, Wong AD, Gerecht S, Searson PC. Review: in vitro microvessel models. Lab Chip 2015; 15: 4242-4255.
[35] Potente M, Gerhardt H, Carmeliet P. Basic and therapeutic aspects of angiogenesis. Cell 2011; 146: 873-887.
[36] Shibata R, Ouchi N, Ohashi K, Murohara T. The role of adipokines in cardiovascular disease. J Cardiol 2017; 70: 329-334.
[37] Liu J, Butler KR, Buxbaum SG, Sung JH, Campbell BW, Taylor HA. Leptinemia and its association with stroke and coronary heart disease in the Jackson heart study. Clin Endocrinol (Oxf) 2010; 72: 32-37.
[38] Artwohl M, Roden M, Hölzenbein T, Freudenthaler A, Waldhäusl W, Baumgartner-Parzer SM. Modulation by leptin of proliferation and apoptosis in vascular endothelial cells. Int J Obes 2002; 26: 577-580.
[39] Sierra-Honigmann MR, Nath AK, Murakami C, García-Cardeña G, Papapetropoulos A, Sessa WC, Madge LA, Schechner JS, Schwabb MB, Polverini PJ, Flores-Riveros JR. Biological action of leptin as an angiogenic factor. Science 1998; 281: 1683-1686.
[40] Carmeliet P, Moons L, Luttun A, Vincenti V, Compernolle V, De Mol M, Wu Y, Bono F, Devy L, Beck H, Scholz D, Acker T, DiPalma T, Dewerchin M, Noel A, Stalmans I, Barra A, Blacher S, VandenDriessche T, Ponten A, Eriksson U, Plate KH, Foidart JM, Schaper W, Charnock-Jones DS, Hicklin DJ, Herbert JM, Collen D, Persico MG. Synergism between vascular endothelial growth factor and placental growth factor contributes to angiogenesis and plasma extravasation in pathological conditions. Nat Med 2001; 7: 575-83.
[41] Bell SE, Mavila A, Salazar R, Bayless KJ, Kanagala S, Maxwell SA, Davis GE. Differential gene expression during capillary morphogenesis in 3D collagen matrices: regulated expression of genes involved in basement membrane matrix assembly, cell cycle progression, cellular differentiation and G-protein signaling. J Cell Sci 2001; 114: 2755-73.
[42] Augustin HG, Koh GY, Thurston G, Alitalo K. Control of vascular morphogenesis and ho-

meostasis through the angiopoietin-tie system. Nat Rev Mol Cell Biol 2009; 10: 165-177.
[43] Jones N, Iljin K, Dumont DJ, Alitalo K. Tie receptors: new modulators of angiogenic and lymphangiogenic responses. Nat Rev Mol Cell Biol 2001; 2: 257-67.
[44] Eklund L, Olsen BR. Tie receptors and their angiopoietin ligands are context-dependent regulators of vascular remodeling. Exp Cell Res 2006; 312: 630-641.
[45] Daly C, Pasnikowski E, Burova E, Wong V, Aldrich TH, Griffiths J, Ioffe E, Daly TJ, Fandl JP, Papadopoulos N, McDonald DM, Thurston G, Yancopoulos GD, Rudge JS. Angiopoietin-2 functions as an autocrine protective factor in stressed endothelial cells. Proc Natl Acad Sci U S A 2006; 103: 15491-15496.
[46] Huang CC, Pan WY, Tseng MT, Lin KJ, Yang YP, Tsai HW, Hwang SM, Chang Y, Wei HJ, Sung HW. Enhancement of cell adhesion, retention, and survival of HUVEC/cbMSC aggregates that are transplanted in ischemic tissues by concurrent delivery of an antioxidant for therapeutic angiogenesis. Biomaterials 2016; 74: 53-63.
[47] Zhang H, Liu S, Zhu B, Xu Q, Ding Y, Jin Y. Composite cell sheet for periodontal regeneration: crosstalk between different types of MSCs in cell sheet facilitates complex periodontal-like tissue regeneration. Stem Cell Res Ther 2016; 7: 168.
[48] Tindholdt TT, Saidian S, Pripp AH, Tønseth KA. Monitoring microcirculatory changes in the deep inferior epigastric artery perforator flap with laser doppler perfusion imaging. Ann Plast Surg 2011; 67: 139-142.
[49] Tindholdt TT, Saidian S, Tønseth KA. Microcirculatory evaluation of deep inferior epigastric artery perforator flaps with laser Doppler perfusion imaging in breast reconstruction. J Plast Surg Hand Surg 2011; 45: 143-147.
[50] Thorfinn J, Sjöberg F, Lidman D. Perfusion of buttock skin in healthy volunteers after long and short repetitive loading evaluated by laser Doppler perfusion imager. Scand J Plast Reconstr Surg Hand Surg 2007; 41: 297-302.
[51] Zdolsek JM, Droog EJ, Thorfinn J, Lidman D. Laser Doppler perfusion imaging of the radial forearm flap: a clinical study. Scand J Plast Reconstr Surg Hand Surg 2006; 40: 101-105.
[52] Glotzbach JP, Levi B, Wong VW, Longaker MT, Gurtner GC. The basic science of vascular biology: implications for the practicing surgeon. Plast Reconstr Surg 2010; 126: 1528-1538.
[53] Zheng Y, Yi C, Xia W, Ding T, Zhou Z, Han Y, Guo S. Mesenchymal stem cells transduced by vascular endothelial growth factor gene for ischemic random skin flaps. Plast Reconstr Surg 2008; 121: 59-69.
[54] Bleiziffer O, Hammon M, Naschberger E, Lipnik K, Arkudas A, Rath S, Pryymachuk G, Beier JP, Stürzl M, Horch RE, Kneser U. Endothelial progenitor cells are integrated in newly formed capillaries and alter adjacent fibrovascular tissue after subcutaneous implantation in a fibrin matrix. J Cell Mol Med 2011; 15: 2452-2461.
[55] Pedersen TO, Blois AL, Xue Y, Xing Z, Sun Y, Finne-Wistrand A, Lorens JB, Fristad I, Leknes KN, Mustafa K. Mesenchymal stem cells induce endothelial cell quiescence and promote capillary formation. Stem Cell Res Ther 2014; 5: 1-10.
[56] Jain RK, Au P, Tam J, Duda DG, Fukumura D. Engineering vascularized tissue. Nat Biotechnol 2005; 23: 821-823.

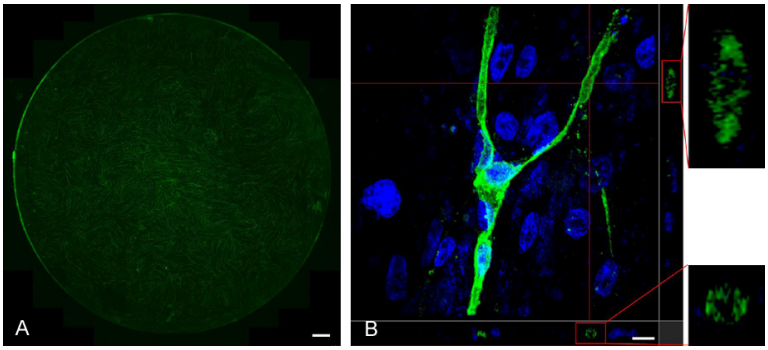


**Figure S1.** A. Mosaic image of PHCS at day 14. Green: CD31, Bar: 1 mm. B. Lumen structure (red rectangle) of PHCS at day 14. Green: CD31, Blue: DAPI, Bar: 10 μm.

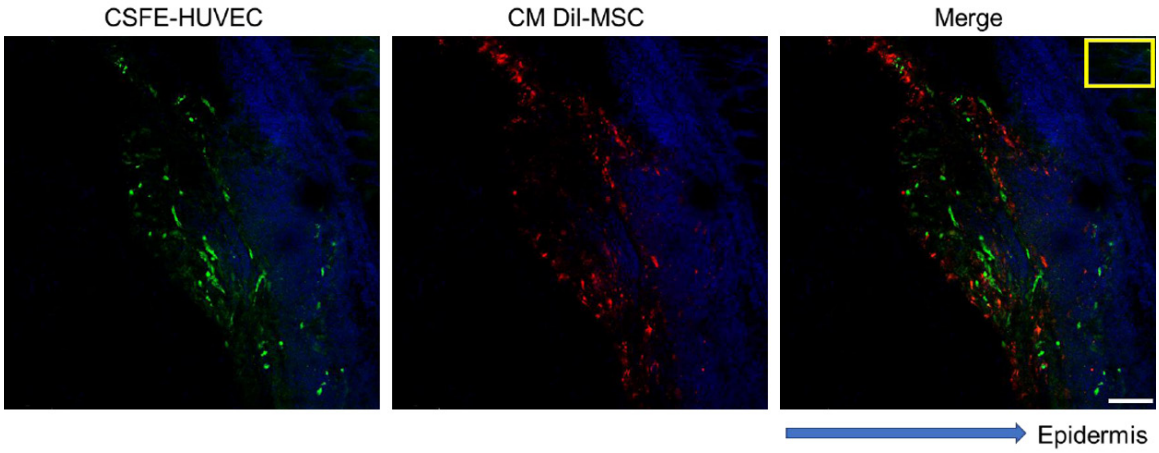


**Figure S2.** Frozen section of tissues from PHCS subcutaneous implantation model at day 7. Green: CSFE-HUVEC, Red: CM Dil-MSC, Blue: DAPI. The yellow box represents the reticular dermis. These images indicated the PHCS surviving for 7 days *in vivo*. Bar: 10 μm.